# HRTEM Investigation of Silicon Nitride Powder Coated with Yttrium Oxide-Precursor

I. J. Davies♦, B. Djuricic, and S. Pickering
*Institute for Advanced Materials, The Netherlands*
and
J. Th. M. De Hosson
*Technische Fysica, Rijksuniversiteit Groningen, The Netherlands*

(Received: Feb. 4, 1997 Accepted: Feb. 19, 1997)

## Abstract

Ceramic matrix composites based on silicon nitride ($Si_3N_4$) are potential candidates for use as high-temperature structural materials. However, the high melting point and low self-diffusion coefficient of $Si_3N_4$ makes fabrication difficult without the addition of a sintering aid such as yttrium oxide ($Y_2O_3$) or aluminium oxide ($Al_2O_3$). Addition of sintering aid through mechanical mixing does not produce homogeneous distribution on the microscale and results in poor control of the sintered $Si_3N_4$ intergranular phases which decreases the oxidation resistance and mechanical properties of such ceramics. An improved method for homogeneous distribution of sintering aid might involve the coating of each ceramic powder particle with a small amount of sintering aid - techniques previously proposed include precipitation from metal salts or metal hydroxides, and electrostatic deposition from a colloidal suspension.

In this study, $Si_3N_4$ powders were coated with 5 wt.% $Y_2O_3$-precursor using a chemical precipitation technique and calcined up to 1400 °C in nitrogen or argon. Investigations using transmission electron microscopy (TEM) and high resolution transmission electron microscopy (HRTEM) were carried out in order to determine the dependence of coating morphology and atomic structure on calcination conditions. Energy dispersive X-ray spectroscopy (EDS) and X-ray diffraction (XRD) were also utilised to determine the dependence of the amount of yttrium and phases present on processing conditions.

It was concluded from EDS observations that $Y_2O_3$-precursor was successfully deposited onto the surface of $Si_3N_4$ whilst direct observation from HRTEM indicated the precursor to consist initially of discrete hemispherical nanocrystalline particles (with typical dimensions 10-100 nm) which were unaffected by calcination at 600 °C in nitrogen. However, calcination at 1400 °C in nitrogen or argon resulted in partial sintering of the coated powder together with crystallisation of the $Y_2O_3$-precursor.

## 1. Introduction

Current materials for use in high strength structural applications at 1000 °C comprise chiefly of nickel-based alloys whilst operating temperatures of 1100 °C require the use of single-crystal nickel-based alloys. Applications at these temperatures include those of aerospace engine casings and turbine blades. However, recent emphasis on improved performance and operating efficiency for such applications has led to a demand for increased operating temperatures which may require widespread utilisation of monolithic ceramics.

However, the relatively low self-diffusion of most ceramics below their decomposition temperature[1] generally necessitates use of small amounts (typically <5 wt.%) of sintering aid which reacts with the amorphous layer (mostly $SiO_2$ together with some $Si_2N_2O$)[2] formed on $Si_3N_4$ and SiC particles exposed to the atmosphere and allows sintering to proceed via a liquid phase. For the silicon nitride ($Si_3N_4$) and silicon carbide (SiC) group of ceramics, sintering aids include aluminium oxide ($Al_2O_3$), aluminium nitride (AlN), and rare earth oxides such as yttrium oxide ($Y_2O_3$)[3-7]. However, use of sintering aids promotes formation of amorphous intergranular phases in the final ceramic which often limit high temperature structural use due to grain boundary shearing and reduced oxidation resistance[8,9].

It is believed that improved high temperature properties for these ceramics may be achieved through reducing the proportion of sintering aid present in the green body together with production of intergranular phases in the final ceramic which are more resistant to oxidation, e.g., $Y_2Si_2O_7$. Deposition of a small amount of sintering aid on the surface of each ceramic particle would significantly reduce the proportion of sintering aid required compared to the present technique of mechanically mixing ceramic powder and sintering aid prior

---

♦ Corresponding author. Present address: Sun Pearl Jindaiji 205, 4-8-6 Jindaiji-Motomachi, Chofu Shi, Tokyo 182, Japan
(e-mail: yasuda_davies@msn.com)

to densification. Deposition techniques also have the benefit of a relatively homogeneous distribution of intergranular phases in the final ceramic. Methods utilised to deposit sintering aid on ceramic particles include in-situ precipitation and co-precipitation from metal salts[10,11] or metal alkoxides[12-16], electrostatic deposition of a colloidal sintering agent[17], and precipitation from nitrate compounds in the presence of urea[18]. However, microstructural investigation at the atomic level for this family of coating techniques has been extremely limited.

The present investigation was carried out to determine the microstructure of nano-coated $Y_2O_3$-precursor deposited onto $Si_3N_4$ powder particles using forced hydrolysis of an aqueous solution of yttrium nitrate ($Y(NO_3)_3$) in the presence of urea ($CON_2H_4$). Techniques utilised included high resolution transmission electron microscopy (HRTEM), transmission electron microscopy (TEM), energy dispersive X-ray spectroscopy (EDS), and X-ray diffraction (XRD).

## 2. Experimental Procedure

The $Si_3N_4$ powder used in this experiment consisted of 95 % α- and 5 % β-phase with equiaxed particles of size 0.1-0.3 μm and a specific surface area of 11.1 $m^2g^{-1}$ (UBE SN-E-10, Ube Industries Ltd., Japan). The yttrium nitrate compound utilised was yttrium nitrate hexahydrate ($Y(NO_3)_3.6H_2O$) (Jannsen Chemicals, Reagent Grade) with an amount equivalent to 5 wt.% $Y_2O_3$ being used.

The technique utilised to coat the $Si_3N_4$ particles is detailed elsewhere[18,19] but essentially consisted of an aqueous solution of $CON_2H_4$ and $Y(NO_3)_3$ adjusted to a pH of 2.0-2.5 with nitric acid ($HNO_3$) to which the $Si_3N_4$ particles were added. The solution was then heated to 86 °C under constant agitation for 1 hour during which time the $CON_2H_4$ decomposed and increased the pH of the solution resulting in precipitation and deposition of an unspecified $Y_xO_yH_z$ compound onto the $Si_3N_4$ surface. After washing and drying at 80-90 °C for 12 hours the powders were calcined for 2 hours under one of the following regimes:

(i) 600 °C and nitrogen atmosphere,
(ii) 1400 °C and nitrogen atmosphere, or
(iii) 1400 °C and argon atmosphere.

Samples of coated $Si_3N_4$ powder were prepared for HRTEM and TEM by ultrasonically dispersing the powder in isopropanol for 5 minutes after which a small droplet of the suspension was placed onto a carbon filmed grid, followed by evaporation of the isopropanol.

HRTEM was carried out using a JEOL 4000EX/II (point resolution 1.65 Å) at 400 kV with images being recorded on negative film at magnifications between 3-4 × $10^5$. Sections of the negative were then digitised with a CCD camera (Kodak Megaplus model 1.4 (1322 × 1035 pixels); 60 mm f2.8 AF Micro Nikkor lens) and further enhanced using image analysis software running on a personal computer. Due to the specimen preparation technique, all HRTEM bright field (BF) images contained an amorphous background image due to the carbon film.

TEM utilised a JEOL 200CX at 200 kV fitted with EDS (Edax 9100, Edax Laboratories). Selected specimens were placed in a graphite holder and rotated so as to be 45° from both the incident electron beam and EDS detector. The electron beam was focused onto single powder particles with an analysis time of 500 seconds being used and results being averaged from a minimum of 5 separate particles.

XRD of coated powders was carried out on a Philips PW173 X-ray diffractometer at 50 kV and 40 mA using CuKα radiation and silicon powder as an internal standard. Diffraction patterns were recorded for the range $2\Theta = 10$-80°.

## 3. Results and Discussion

Figure 1 illustrates the edge of a typical uncoated $Si_3N_4$ particle observed in this investigation, with negligible amorphous surface layer being apparent. Although previous researchers[2] had suggested an oxide layer of typically 3-5 nm to be present on the surface of $Si_3N_4$ particles, it is also known that residual fluorine may decrease the surface oxygen content such that amorphous surface layers of <1 nm thickness may be feasible. Thus, one explanation for the lack of a distinct amorphous surface layer in the present $Si_3N_4$ particles would be a relatively high fluorine content but

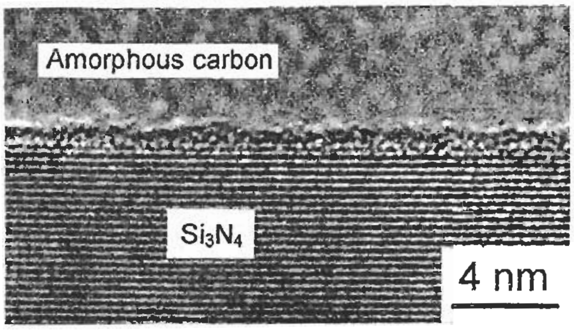

**Fig. 1** HRTEM micrograph illustrating the surface of as-received $Si_3N_4$ with negligible amorphous surface (oxide) layer.

this has not been confirmed. Although most uncoated $Si_3N_4$ particles exhibited no distinct amorphous surface layer, it should be stressed that surface (oxide) layers of several nanometres thickness were occasionally observed indicating that surface oxygen content may vary from particle to particle.

Observation of coated $Si_3N_4$ powder prior to calcination indicated (suspected) $Y_2O_3$-precursor to be present, though not continuously distributed on the $Si_3N_4$ surface but instead consisting of discrete hemispherical particles. Such a result is consistent with the low proportion of $Y_2O_3$-precursor present in this system together with previous researchers who suggested that only a portion of the $Si_3N_4$ surface is available for nucleation of $Y^{3+}$ ions due to the presence of silylamine ($SiNH_2$ or SiNH) groups[11].

Figure 2 illustrates a typical $Y_2O_3$-precursor particle attached to the surface of $Si_3N_4$ powder with the particle having approximate dimensions of 50 nm diameter and 12 nm thickness. Coating particles were generally noted with diameters in the range 10-100 nm whilst thickness varied to a lesser extent (5-20 nm). From Figure 2(b) it may be observed that $Y_2O_3$-precursor particles under these conditions possessed nanocrystalline structures whilst highly strained lattice structures parallel to the particle outer surface were often noted. Although the majority of $Y_2O_3$-precursor particles were approximately hemispherical in shape, in a small number of cases the $Y_2O_3$-precursor particle showed itself as a highly strained lattice (<20 atomic layers thick) running almost parallel to the $Si_3N_4$ surface with a length (diameter) of >100 nm (Figure 3). For this case the structure was crystalline to a far greater extent than that observed in Figure 2(b) suggesting a different formation mechanism.

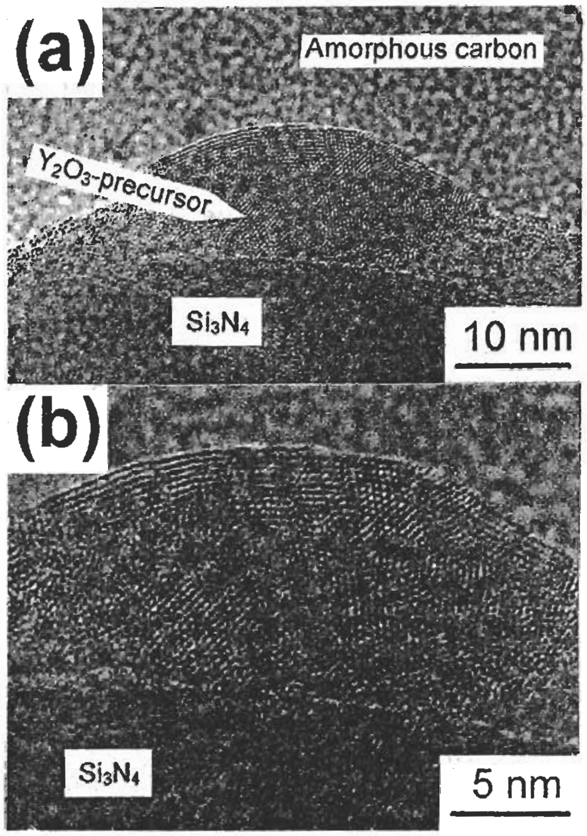

**Fig. 2** HRTEM micrographs illustrating a nanocrystalline $Y_2O_3$-precursor hemispherical particle attached to the surface of uncalcined $Si_3N_4$.

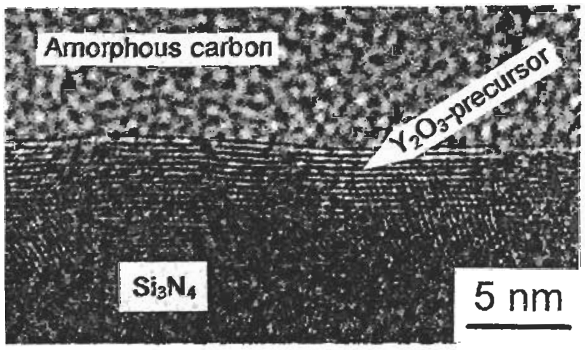

**Fig. 3** HRTEM micrograph showing a $Y_2O_3$-precursor particle with highly strained lattice structure running parallel to the $Si_3N_4$ surface.

An EDS spectrum for uncalcined coated $Si_3N_4$ powder has been presented in Figure 4(b) whilst a background reference spectrum (taken in the vicinity of coated $Si_3N_4$ particles) is given in Figure 4(a). The EDS spectrum of the coated $Si_3N_4$ particle (Figure 4(b)) possessed addition peaks not present in Figure 4(a) which were attributed to Si and Y transitions. From this result it was concluded that Y co-exists with Si with the most likely scenario being that $Y_2O_3$-precursor materials (of unknown composition) were present on the $Si_3N_4$ surface in the form of mainly hemispherical particles. Comparison between Si and Y peaks in Figure 4(b) gave calculated atomic percentages of 98.0 (+/–0.8) % and 2.0 (+/–0.8) %, respectively, which were in excellent agreement with predicted values of 97.9 % Si and 2.1 % Y assuming complete deposition of precipitated $Y_2O_3$-precursor onto $Si_3N_4$. Thus, this technique is shown to be highly efficient at coating ceramic particles with small amounts of sintering aid precursor. This result, combined with the existence of $Y_2O_3$-precursor particles on the $Si_3N_4$ surface, indicates the most probable coating scenario to have been heterogeneous nucleation of $Y_2O_3$-precursor on the $Si_3N_4$ surface[18].

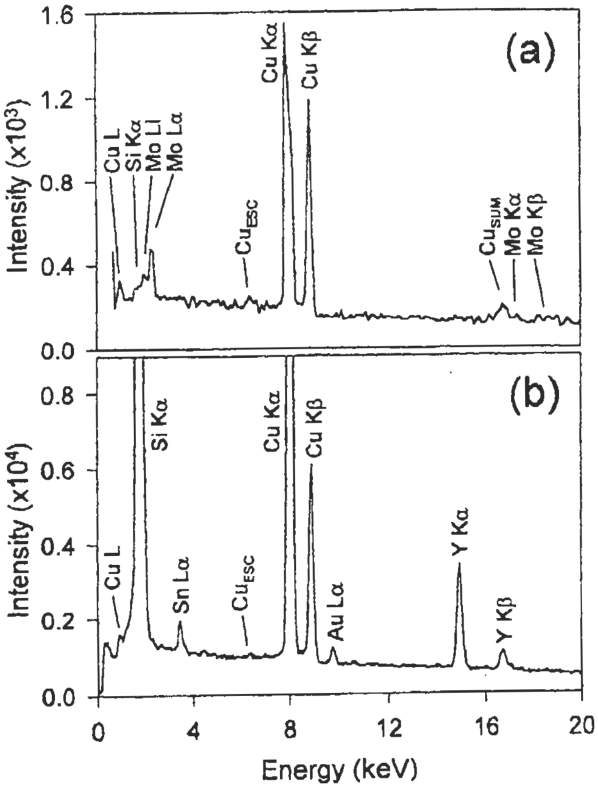

**Fig. 4** EDS spectra for uncalcined coated $Si_3N_4$ powder: (a) background reference, and (b) powder particle.

The XRD spectrum of coated $Si_3N_4$ prior to calcination yielded only peaks assigned to $Si_3N_4$. Such a result would be expected taking into account the small amount of $Y_2O_3$-precursor present and its nanocrystalline morphology.

HRTEM micrographs illustrating the structure of $Y_2O_3$-precursor particles on the surface of $Si_3N_4$ powder calcined for 2 hours at 600 °C in $N_2$ have been presented in Figure 5 and Figure 6. The structure of the $Y_2O_3$-precursor particle in Figure 5 is essentially nanocrystalline and similar to that seen previously for uncalcined coated powder (Figure 2). It would appear that the alcination condition employed (2 hrs/600 °C/$N_2$) was not sufficient to initiate ordering of the $Y_2O_3$-precursor and this is confirmed from Figure 6 which presents a $Y_2O_3$-precursor particle with an almost amorphous structure.

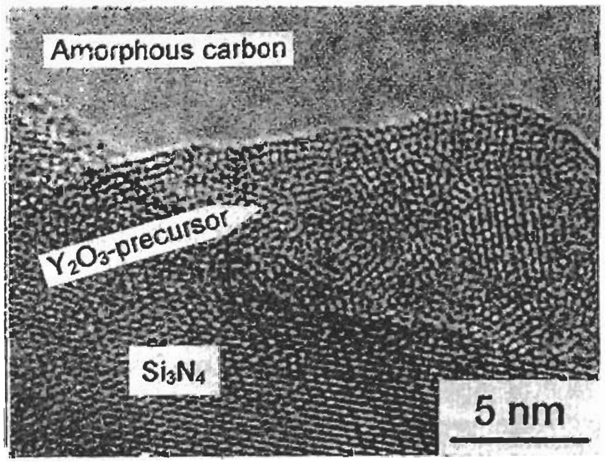

**Fig. 5** HRTEM micrograph illustrating a nanocrystalline $Y_2O_3$-precursor particle on the surface of $Si_3N_4$ powder calcined for 2 hours at 600 °C in nitrogen.

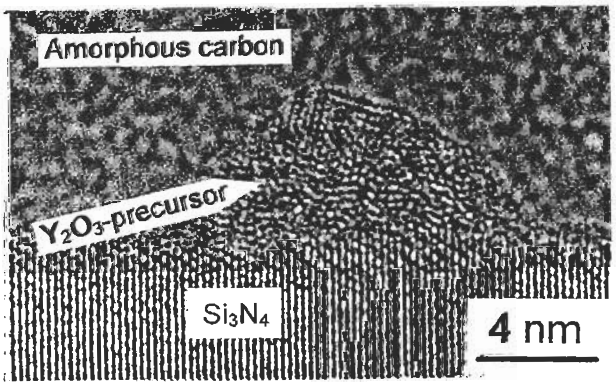

**Fig. 6** HRTEM micrograph showing an amorphous $Y_2O_3$-precursor particle on the surface of $Si_3N_4$ powder calcined for 2 hours at 600 °C in nitrogen.

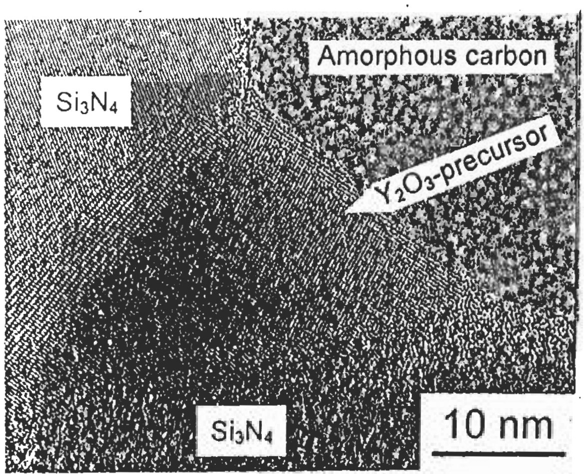

Fig. 7 HRTEM micrograph illustrating crystallised $Y_2O_3$-precursor between $Si_3N_4$ powder particles calcined for 2 hours at 1400 °C in nitrogen.

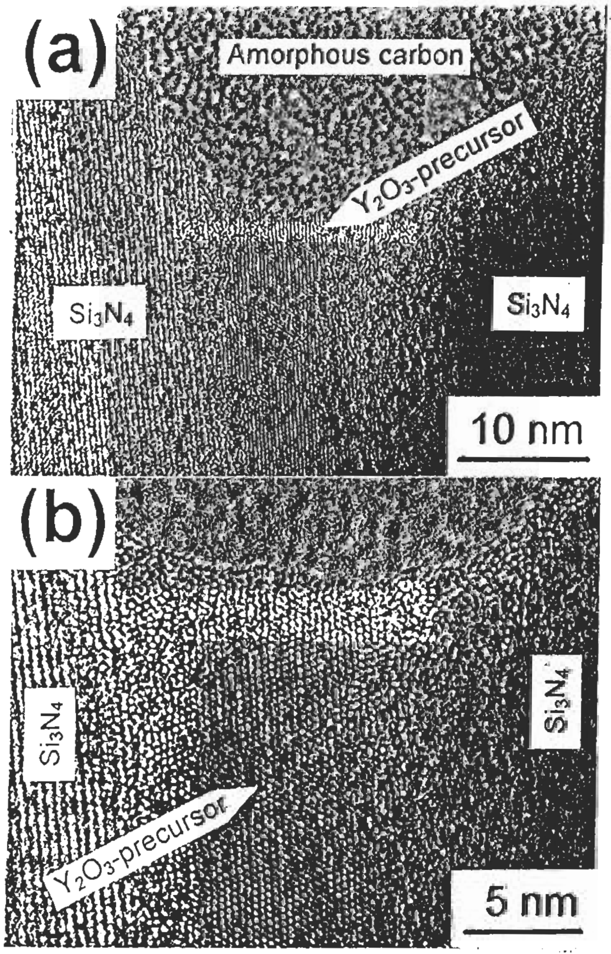

Fig. 8 HRTEM micrographs showing crystallised $Y_2O_3$-precursor between $Si_3N_4$ powder particles calcined for 2 hours at 1400 °C in argon.

In order to promote ordering of the $Y_2O_3$-precursor particles, coated $Si_3N_4$ powder was calcined at 1400 °C in $N_2$ or Ar with microstructural characteristics of the resultant $Y_2O_3$-precursor being significantly different compared to that observed earlier (i.e., individual $Y_2O_3$-precursor hemispherical particles adhered to the $Si_3N_4$ surface). After calcination at 1400 °C in $N_2$ or Ar, the $Y_2O_3$-precursor possessed a well-defined crystal structure and preferentially positioned at the "neck" of partially sintered $Si_3N_4$ particles (Figure 7 and Figure 8).

Such observations may be explained through the scenario of low temperature liquid phase production derived from the reaction of $Y_2O_3$-precursor particles with available oxygen on the $Si_3N_4$ surface. Such liquid phases are known to occur in the presence of $Y_2O_3$ sintering aid and might also be expected to promote dissolution of $Si_3N_4$ (though partial dissolution is a more realistic scenario in the present case taking into account the relatively low temperature and short time utilised). Surface tension effects would tend to concentrate the liquid phase at the contact point or "neck" of $Si_3N_4$ particles. A probable next step would involve epitaxial deposition of $Si_3N_4$ or Y-Si-O-N from the liquid phase onto the remaining $Si_3N_4$ particle followed by crystallisation of a $Y_2O_3$-rich phase at the "neck" of $Si_3N_4$ particles during cooling. Further evidence indicating the formation of $Y_2O_3$-rich crystalline phases under these calcination conditions may be inferred from the XRD spectrum for coated $Si_3N_4$ calcined for 2 hours at 1400 °C in $N_2$ (Figure 9). In addition to prominent peaks attributed to α- and β-

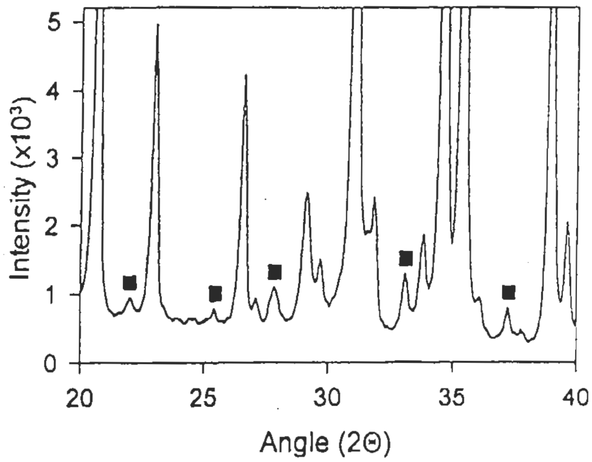

Fig. 9 XRD spectrum of coated $Si_3N_4$ powder after calcination for 2 hours at 1400 °C in nitrogen. All peaks are identified as $Si_3N_4$ except those labeled "■" which are attributed to the $Y_2O_3$-rich crystalline phase.

$Si_3N_4$, lower intensity peaks were also present within the 2Θ range 20-40° at positions identical to those expected for several compositions within the Y-Si-O-N phase diagram. However, the relatively large full width at half maximum (FWHM) of the $Y_2O_3$-rich peaks together with the superimposition of a large number of $Si_3N_4$ peaks in the same 2Θ range precluded identification of the exact phase(s) present, though likely candidates included $Y_2O_3$. The relatively large FWHM of $Y_2O_3$-rich peaks was at least partially attributed to variations in surface oxygen concentration between individual $Si_3N_4$ particles resulting in $Y_2O_3$-rich crystalline regions with different chemical composition and/or phases.

## 4. Conclusions

(i) $Y_2O_3$-precursor was successfully deposited onto the surface of $Si_3N_4$ with negligible loss of Y either during the deposition procedure or subsequent calcination regimes.

(ii) $Y_2O_3$-precursor on the uncalcined powder generally exhibited itself as hemispherical nanocrystalline particles. The diameter of individual $Y_2O_3$-precursor particles was in the range 10-100 nm whilst the thickness was limited to 5-20 nm. A calcination of 2 hours at 600 °C in $N_2$ had no effect on the $Y_2O_3$-precursor structure.

(iii) Calcination for 2 hours at 1400 °C in $N_2$ or Ar produced $Y_2O_3$-precursor with a well-defined crystal structure preferentially positioned at the "neck" of partially sintered $Si_3N_4$ particles. These characteristics were attributed to formation of a liquid phase involving the $Y_2O_3$-precursor and $Si_3N_4$ surface oxide layer.

## Acknowledgments

This research was carried out as part of the European Commission Research and Development Programme. Two of the authors (IJD and BD) were supported during this work as visiting scientists by the European Commission.

## References

1. M. H. Lewis and R. J. Lumby, "Nitrogen ceramics: liquid phase sintering", Powder Metallurgy, **26(2)** 73-81 (1983)
2. M. N. Rahaman, Y. Boiteux, and L. C. De Jonghe, "Surface characterization of silicon nitride and silicon carbide powders", Amer. Ceram. Soc. Bull., **65** 1171-1176 (1986)
3. G. Wotting and G. Ziegler, "Powder characteristics and sintering behaviour of $Si_3N_4$ powders", Powder Metallurgy International, **18(1)** 25-32 (1986)
4. R. A. Cutler and T. B. Jackson, "Liquid phase sintered silicon carbide", in Ceramic materials and components for engines: Proceedings of the 3rd international symposium (Las Vegas, NV, U.S.A., 1988), 309-318, edited by V. J. Tennery, American Ceramic Society, Westerville, OH, U.S.A. (1989)
5. L. Cordrey, D. E. Niesz, and D. J. Shanefield, "Sintering of silicon carbide with rare-earth oxide additions", Ceram. Trans., 7 618-636 (1990)
6. M. A. Mulla and V. D. Krstic, "Low-temperature pressureless sintering of β-silicon carbide with aluminium oxide and yttrium oxide additions", Amer. Ceram. Bull., **70** 439-443 (1991)
7. R. R. Lee and W. C. Wei, "Fabrication, microstructure, and properties of SiC-AlN ceramic alloys", Ceram. Eng. Sci. Proc., **11** 1094-1121 (1990)
8. M. H. Lewis and P. Barnard, "Oxidation mechanisms in Si-Al-O-N ceramics", J. Mater. Sci., **15** 443-448 (1980)
9. D. M. Mieskowski and W. A. Sanders, "Oxidation of silicon nitride sintered with rare-earth oxide additions", J. Amer. Ceram. Soc., **68(7)** C160-163 (1985)
10. T. M. Shaw and B. A. Pethica, "Preparation and sintering of homogeneous silicon nitride green compacts", J. Amer. Ceram. Soc., **69(2)** 88-93 (1986)
11. J. -S. Kim, H. Schubert, and G. Petzow, "Sintering of $Si_3N_4$ with $Y_2O_3$ and $Al_2O_3$ added by co-precipitation", J. Europ. Ceram. Soc., **5** 311-319 (1989)
12. T. -I. Mah, K. S. Mazdiyasni, and R. Ruh, "Characterisation and properties of hot-pressed $Si_3N_4$ with alkoxy-derived $CeO_2$ or $Y_2O_3$ as sintering aids", Amer. Ceram. Soc. Bull., **58(9)** 840-844 (1979)
13. C. -M. Wang and F. L. Riley, "Alumina-coating of silicon nitride powder", J. Europ. Ceram. Soc., **10** 83-93 (1992)
14. M. Kulig, W. Oroschin, and P. Greil, "Sol-gel coating of silicon nitride with Mg-Al oxide sintering aid", J. Europ. Ceram. Soc., **5** 209-217 (1989)

15. M. Omori and H. Takei, "Preparation of pressureless-sintered SiC-$Y_2O_3$-$Al_2O_3$", J. Mater. Sci., **23** 3744-3749 (1988)
16. H. K. Lee and K. Y. Kim, "Synthesis of $Al_2O_3$ coated SiC composite powder", J. Mater. Sci. Lett., **13** 1149-1150 (1994)
17. E. Liden, M. Persson, E. Carlstrom, and R. Carlsson, "Electrostatic adsorption of a colloidal sintering agent on silicon nitride particles", J. Amer. Ceram. Soc., **74(6)** 1335-1339 (1991)
18. A. K. Garg and L. C. De Jonghe, "Microencapsulation of silicon nitride particles with yttria and yttria-alumina precursors", J. Mater. Res., **5(1)** 136-142 (1990)
19. B. Djuricic, I. J. Davies, S. Pickering, D. McGarry, E. Bullock, M. Verwerft, P. M. Bronsveld, and J. Th. M. De Hosson, "Study of particle coatings for the design of intergranular phases in engineering ceramics", Silicates Industriels, **60(7-8)** 203-210 (1995)